

Supplementary Information

An image-driven drop-on-demand system

Camille Girabawe^a, Seth Fraden^{a*}

^a*Department of Physics, Brandeis University, 415 South Street, Waltham, MA 02453, USA*

Appendix A. Fabrication of the silicon master for the PDMS device

In order to fabricate the PDMS chip with pneumatic valves using soft lithography techniques, two different silicon masters were required.

A.1. Flow layer master

The master for the flow layer was made with two different heights as sketched in Figure A.1.A. In the first step, positive photoresist SPR220 (purchased from MicroChem) was used to produce rounded channels with a maximum height of 20 μm and width 80 μm . The rounded channels improved sealing of the channel using push-up valves. SPR220 was spin-coated on a blank silicon wafer (Silicon 76.2 mm purchased from UniversityWafer, Inc), soft baked for 2 minutes at 65°C and 5 minutes at 105°C. It was then overlaid with a photomask containing black features on a transparent background and exposed to the ultra-violet (UV) light (4.5mJ/cm²) for 30 seconds. After the exposure, the silicon wafer was developed using AZ400 (purchased from Clariant) dissolved in water at a ratio of 1:2 (AZ400:water) for about 3 minutes and rinsed with pure water to remove all of the resist that was exposed to UV light. Finally, the master could be hard baked at 200°C for 2 hours to partially melt the resist hence transforming rectangular into rounded corners.

In the second step, SU8-3035 (purchased from MicroChem) was used to make rectangular channels with height of 50 μm and width 150 μm . SU8 was poured and coated on the master obtained from the first step. The master was then soft baked for 1 minute at 65°C, 5 minutes at 95°C and 1 minute back to 65°C. It was then overlaid with a photomask containing transparent features on a black background and UV-exposed for 1 minute. The master was then baked at same temperature steps as in the soft baking. After the post-exposure baking, the master was developed using propylene glycol monomethyl ether acetate (PGMEA) for 3 minutes and then rinsed with isopropanol to remove all of the resist that was not UV-exposed. Finally, the master was

* Corresponding author. Tel.: +0-000-000-0000 ; fax: +0-000-000-0000 .
E-mail address: fraden@brandeis.edu.

hard baked at 180°C for 2 hours (see Figure A.1.A).

A.2. Control layer master

The control layer master was fabricated similarly to the fabrication of the second step of the flow layer to produce channels 50µm high (see Figure A.1.B).

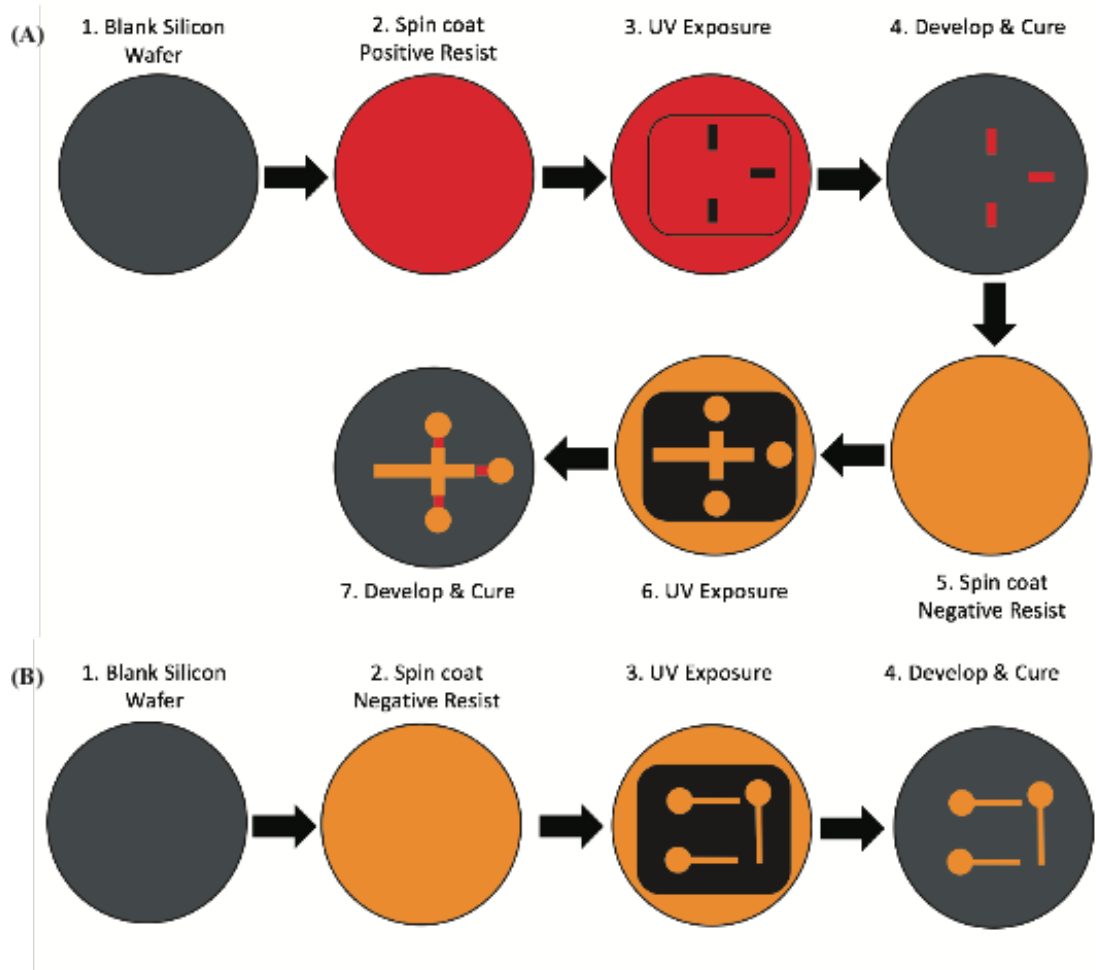


Figure A.1 Schematics illustrating the fabrication of (A) the flow layer: positive resist (SPR220) was (1) spin coated on a blank silicon wafer and soft baked, (2) UV-exposed using a photomask with dark features printed on a transparent background, (3) developed and hard baked to cure. Next, (4), the negative resist (SU8) was spin coated on the master and soft baked, (5) UV-exposed using a photomask with transparent features on an opaque background and then (6) developed and hard baked to cure. (B) The control layer master is fabricated using a blank silicon wafer and starting the process from phase 4 of the flow layer master.

Appendix B. Fabrication of the PDMS device

To fabricate the PDMS chip, silicon masters fabricated in the previous section were used. First, the liquid Polydimethylsiloxane (Dow Corning Sylgard 184 Silicone Encapsulant Kit purchased from Ellsworth) was mixed with its crosslinker at a ratio of 10:1 (PDMS:Crosslinker). Part of the mixture was poured onto the flow layer master, held in a petri dish, and left in a vacuum machine for 10 - 15 minutes to suck out all air bubbles trapped in the PDMS during the mixing. After degassing, the Petri dish was left in the oven at 72°C for 1 hour to cure the PDMS. In the meantime, another part of the PDMS was spin coated onto the surface of the control layer master (fabricated with 50µm high features) to produce a PDMS layer of total height 70µm, that is, a 20µm thin layer on top of channels. The master with the layer of the PDMS was then put on a hot plate at 85°C for 1 hour to cure and harden the PDMS. With both parts of PDMS cured, the flow layer was pilled off the master and holes are punched. Then, it was plasma-bonded on top of the control layer (which remain cured and attached to the master). The two PDMS layers bonded together, were left in the oven at 72°C for an hour to strengthen bonds. After, it was then safe to pill the two PDMS layers off the control layer, punch necessary holes and bind it to a flat PDMS substrate using plasma again (see Figure B.1).

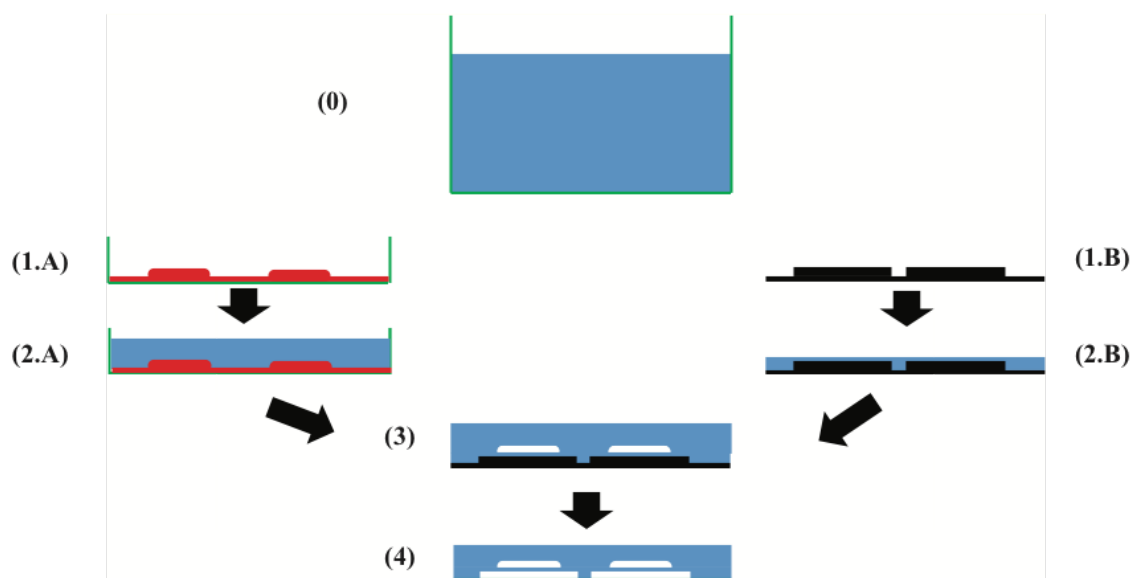


Figure B.2 Figure B.2 Fabrication of the PDMS chip. (0) A solution of PDMS and crosslinker (10:1) was prepared. (1) Wafers are also prepared by (.A) putting the flow layer master in a Petri dish and (.B) mounting the control layer master on a spin coating machine. (2) The PDMS solution is then (.A) poured onto the master in the Petri dish, put in a vacuum machine to remove air bubbles and left in the oven at 72°C for 1 hour to cure the PDMS. In the meantime, (.B) PDMS is spin coated to achieve a 70µm thin layer and left on a hot plate at 85°C for an hour. (3) The two parts cured, the flow layer PDMS is pilled off the master, holes punched and plasma bonded on top of the control layer (remaining un-pilled on the master). The bonded layers are then left in the oven to cure for 1 hour. (4) The two bonded layers are pilled off the master, holes punched and bonded to a flat PDMS substrate.

Appendix C. Measurement of the drop's volume

Consider a drop inside a cylindrical capillary of inner diameter $d = 2r$ (see Figure C.1). The drop has a shape of a sphero-cylinder that can be divided into three parts: the left cap with thickness $t_{left} = x_1 - x_0$, the central rectangular cylinder of length $l = x_2 - x_1$ and the right cap of thickness $t_{right} = x_3 - x_2$, symmetrically identical to

the left cap. The left cap is a part of sphere of radius R such that for every point on the cap surface

$$R^2 = y^2 + (R - x)^2 \quad (\text{C.1})$$

where x is the horizontal distances measured from the leftmost point of the cap to the point of interest on the surface of the drop. The volume of the drop can be calculated as an integral

$$V = \int_{x_0=0}^{x_1=t_{left}} \pi y^2 dx + \int_{x_1}^{x_2} \pi y^2 dx + \int_{x_2}^{x_3} \pi y^2 dx \quad (\text{C.2})$$

Using equation (C.2),

$$V_{left} = \pi \int_{x_0=0}^{x_1=t_{left}} (2Rx - x^2) dx = \pi \left(R t_{left}^2 - \frac{t_{left}^3}{3} \right) \quad (\text{C.3})$$

by symmetry

$$V_{right} = \pi \left(R t_{right}^2 - \frac{t_{right}^3}{3} \right) \quad (\text{C.4})$$

while

$$V_{middle} = \pi \int_{x_1}^{x_2} y^2 dx = \pi r^2 l \quad (\text{C.5})$$

The volume of the drop is then calculated as

$$V = \pi t_{left}^2 \left(R - \frac{t_{left}}{3} \right) + \pi r^2 l + \pi t_{right}^2 \left(R - \frac{t_{right}}{3} \right) \quad (\text{C.6})$$

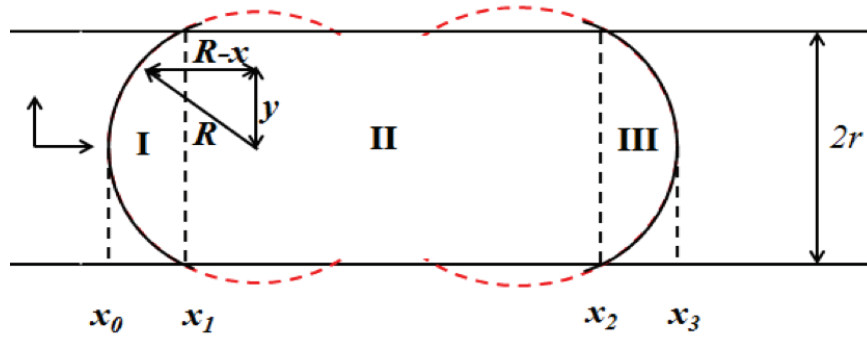


Figure C.1 Schematic illustrating the sphero-cylindrical geometry of a drop inside a cylindrical capillary of radius r . The drop is thought of made with three parts: (I) left cap, (II) central rectangular cylinder and (III) right cap assumed to be symmetrically identical to the left cap.

Appendix D. Model to calculate final concentration

Consider a cylindrical glass capillary containing N drops with different initial concentrations of Sodium Chloride (NaCl). Each drop i has known initial salt concentration $c_{i,0}$ and volume $v_{i,0}$. Assuming that the capillary is well sealed and no ions are transported through the oil, the initial difference in salt concentration establishes a chemical potential gradient between drops, which induces diffusion of water molecules from drops with low salt concentration to drops with high salt concentration. Consequently, low concentration drops should shrink while high concentrated drops swell until they all equilibrate with the same final salt concentration. Using Fick's laws of diffusion, we can write $c_{i,0}v_{i,0} = c_{i,f}v_{i,f}$ and calculate the final concentration of each individual drop as

$$c_{i,f} = \frac{c_{i,0}v_{i,0}}{v_{i,f}} \quad (\text{D.1})$$

where $c_{i,f}$ and $v_{i,f}$ are final concentration and volume respectively. In equation (D.1), the final volume is estimated from recorded images. However, we have seen that some drops did not reach equilibrium. It was of our interest to derive a model to predict the final volume and concentration given drops initial volume and concentration.

At equilibrium, all drops should have the same expected final concentration $c = c_{i,f}$ and we can rewrite the equation as $c_{i,0}v_{i,0} = cv_{i,f}$ for $i=1,2,\dots,N$. That is

$$\begin{cases} c_{1,0}v_{1,0} = cv_{1,f} \\ c_{2,0}v_{2,0} = cv_{2,f} \\ c_{3,0}v_{3,0} = cv_{3,f} \\ \dots \\ c_{N-1,0}v_{N-1,0} = cv_{N-1,f} \\ c_{N,0}v_{N,0} = cv_{N,f} \end{cases} \quad (\text{D.2})$$

Which can be transformed by dividing equilibrium equation of the i^{th} drop by that of the $(i-1)^{\text{th}}$ drop

$$\begin{cases} \frac{c_{2,0}v_{2,0}}{c_{1,0}v_{1,0}} = \frac{cv_{2,f}}{cv_{1,f}} \\ \frac{c_{3,0}v_{3,0}}{c_{2,0}v_{2,0}} = \frac{cv_{3,f}}{cv_{2,f}} \\ \dots \\ \frac{c_{N,0}v_{N,0}}{c_{N-1,0}v_{N-1,0}} = \frac{cv_{N,f}}{cv_{N-1,f}} \end{cases} \quad (\text{D.3})$$

equivalent to

$$\begin{cases} \frac{c_{2,0}v_{2,0}}{c_{1,0}v_{1,0}}v_{1,f} - v_{2,f} = 0 \\ \frac{c_{3,0}v_{3,0}}{c_{2,0}v_{2,0}}v_{2,f} - v_{3,f} = 0 \\ \dots \\ \frac{c_{N,0}v_{N,0}}{c_{N-1,0}v_{N-1,0}}v_{N-1,f} - v_{N,f} = 0 \end{cases} \quad (\text{D.4})$$

In addition, the sum of initial volumes should equal to the sum of final volumes V

$$V = v_{1,f} + v_{2,f} + \dots + v_{N,f} = v_{1,0} + v_{2,0} + \dots + v_{N,0} \quad (\text{D.5})$$

Combining equation (D.4) and (D.5), we can solve for expected final volumes as

$$\begin{bmatrix} \frac{c_{2,0}v_{2,0}}{c_{1,0}v_{1,0}} & -1 & 0 & \dots & \dots & 0 \\ 0 & \frac{c_{3,0}v_{3,0}}{c_{2,0}v_{2,0}} & -1 & 0 & \dots & 0 \\ \dots & \dots & \dots & \dots & \dots & \dots \\ 0 & 0 & \dots & \dots & \frac{c_{N,0}v_{N,0}}{c_{N-1,0}v_{N-1,0}} & -1 \\ 1 & 1 & 1 & \dots & 1 & 1 \end{bmatrix} \begin{bmatrix} v_{1,f} \\ v_{2,f} \\ \dots \\ v_{N-1,f} \\ v_{N,f} \end{bmatrix} = \begin{bmatrix} 0 \\ 0 \\ 0 \\ 0 \\ 0 \\ V \end{bmatrix} \quad (\text{D.6})$$

Equation (D.6) was solved in MATLAB to find the expected final volume of each drop given its initial concentration and volume. With this predicted volume, equation (D.1) was used again to calculate the expected final concentration c from which deviations were calculated as

$$\text{relative error} = \frac{c_{i,f} - c}{c} \quad (13)$$

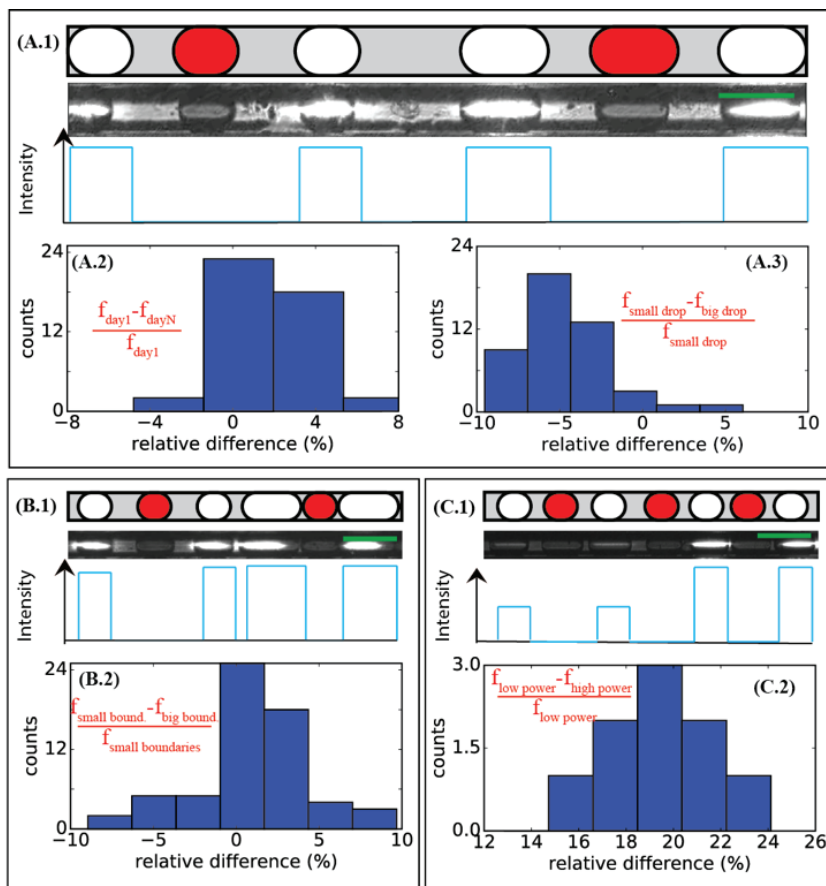


Figure E.1 Control experiments for BZ drops. (A.1, B.1, C.1) First rows are sketches of drops with different sizes inside a cylindrical capillary. White drops are exposed to light to create constant chemical boundary conditions. Red drops are freely oscillating while grey regions represent the oil. The second rows are photographs of capillaries filled with drops as sketched in the first row. The third rows represent light intensity profile used to create boundaries. The green scale bar is $180\mu\text{m}$. Relative difference between frequencies of oscillation of (A.2) drops with same size but generated on different days as shown in (A.1), (A.3) drops with different sizes as shown in (A.1), (B.2) drops with same sizes but bounded with bigger drops as shown in (B.1), (C.2) drops with same size but held at different light intensity as shown in (C.1): half power was used on left side drops compared to those right side. On each figure, the formula used to calculate relative difference is given in red

Appendix E. Control experiments of the Belousov-Zhabotinsky drops

Here, we present control experiments performed in order to investigate how the intrinsic frequency depends on the drop size, boundaries and light intensity. Using the same chemical concentrations and microfluidics techniques as described in the main paper, sequences of drops with different sizes were generated as described in Figure E.1. Frequencies were compared by calculating their relative difference as

$$\text{rd}(i,j) = \frac{f_i - f_j}{f_j} \quad (\text{E.1})$$

where $\text{rd}(i,j)$ is the relative difference between frequencies of drop i and j with relative to drop i .

It was found that increasing the drop size by 1/3 would increase the frequency of oscillation by 5% (Figure E.1.A.3). Furthermore, having a small drop positioned between two big boundary drops didn't change its frequency (Figure E.1.B.2) which implies that the frequency of oscillation is independent of the amount of components diffusing from boundary drops. Finally, the light intensity shone on boundary drops was found to dramatically change the frequency of oscillation of the isolated drop (Figure E.1.C.2). Doubling the light intensity on boundary drops slows down the oscillations of the isolated drop by 20%.

Appendix F. Dynamics of the water exchange between droplets

Here, we present additional data on how concentrations of droplets change as function of the distance between droplets (see Figure F.1).

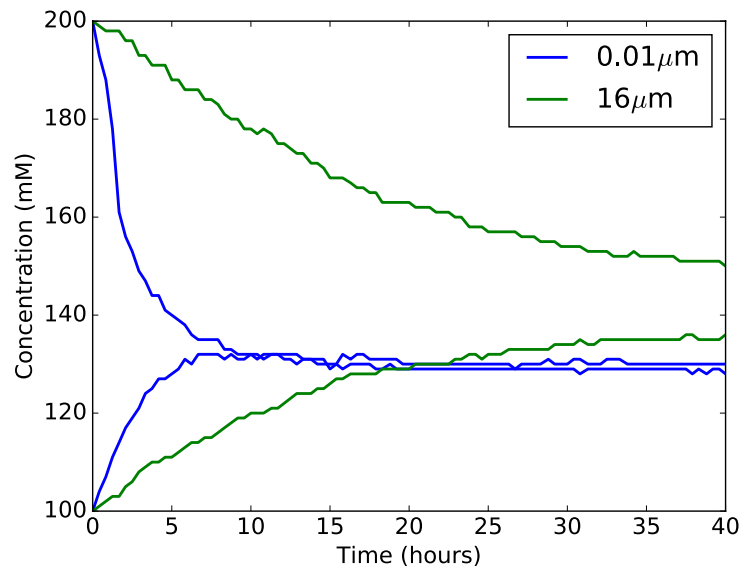


Figure F.1 Change in concentrations as function of the distance between neighbouring drops containing 200mM and 100mM of salt immersed in oil with 4% surfactant. Green and blue represent dynamics of different pairs of neighbouring drops separated by 0.01μm and 16μ respectively.

Appendix G. List of videos

Video1: Drop generation. Scale bar is 700 μm .

Video2: Control of inter-drop separation. Scale bar is 1000 μm .

Video3: Phase contrast video of two drops with initial concentrations of 200mM (left) and 100mM (right). They begin in contact, but the smaller drop moves faster than the bigger drop. Scale bar is 100 μm .

Video4: Region between two drops shows particulates undergoing Brownian motion. Scale bar is 25 μm .